Original Research

Computed tomography-based radiomic model at node level for the prediction of normal-sized lymph node metastasis in cervical cancer

Yujia Liu [a,b,1], Huijian Fan [c,1], Di Dong [a,b,d,1], Ping Liu [c,1], Bingxi He [b,e], Lingwei Meng [a,b], Jiaming Chen [c], Chunlin Chen [c,*], Jinghe Lang [c,f,*], Jie Tian [b,d,g,**]

[a] School of Artificial Intelligence, University of Chinese Academy of Sciences, Beijing 100049, China
[b] CAS Key Laboratory of Molecular Imaging, Institute of Automation, Chinese Academy of Sciences, Beijing 100190, China
[c] Department of Obstetrics and Gynecology, Nanfang Hospital, Southern Medical University, Guangzhou 510515, China
[d] Zhuhai Precision Medical Center, Zhuhai People's Hospital (affiliated with Jinan University), Zhuhai 519000, China
[e] School of Electronic, Electrical and Communication Engineering, University of Chinese Academy of Sciences, Beijing 100049, China
[f] Department of Obstetrics and Gynecology, Peking Union Medical College Hospital, Chinese Academy of Medical Sciences & Peking Union Medical College, No.1 Shuaifuyuan Wangfujing Dongcheng District, Beijing 100730, China
[g] Beijing Advanced Innovation Centre for Big Data-Based Precision Medicine, School of Medicine, Beihang University, Beijing 100191, China

A R T I C L E   I N F O

Keywords:
Cervical cancer
Lymph node metastasis
Radiomics
Preoperative prediction
Classifiers

A B S T R A C T

Purpose: Radiomic models have been demonstrated to have acceptable discrimination capability for detecting lymph node metastasis (LNM). We aimed to develop a computed tomography–based radiomic model and validate its usefulness in the prediction of normal-sized LNM at node level in cervical cancer.

Methods: A total of 273 LNs of 219 patients from 10 centers were evaluated in this study. We randomly divided the LNs from the 2 centers with the largest number of LNs into the training and internal validation cohorts, and the rest as the external validation cohort. Radiomic features were extracted from the arterial and venous phase images. We trained an artificial neural network (ANN) to develop two single-phase models. A radiomic model reflecting the features of two-phase images was also built for directly predicting LNM in cervical cancer. Moreover, four state-of-the-art methods were used for comparison. The performance of all models was assessed using the area under the receiver operating characteristic curve (AUC).

Results: Among the models we built, the models combining the features of two phases surpassed the single-phase models, and the models generated by ANN had better performance than the others. We found that the radiomic model achieved the highest AUCs of 0.912 and 0.859 in the training and internal validation cohorts, respectively. In the external validation cohort, the AUC of the radiomic model was 0.800.

Conclusion: We constructed a radiomic model that exhibited great ability in the prediction of LNM. The application of the model could optimize clinical staging and decision-making.

Introduction

Cervical cancer is the fourth most common cancer in the world and also the fourth most common cause of cancer mortality in women, with approximately 570,000 incident cases and 311,000 deaths in 2018 [1]. Lymph node metastasis (LNM) is one of the most influential prognostic factors in cervical cancer patients. Previous studies have demonstrated that among cervical cancer patients who initially undergo surgery, those without LNM have better 5-year survival rates than those with LNM (80–100% vs 47–78%) [2]. Accordingly, the 2018 revised International Federation of Gynecology and Obstetrics (FIGO) staging system of cervical cancer first included the lymph node (LN) status as a staging criterion. Cervical cancer with lymph node involvement detected at imaging or pathology is categorized as stage IIIC [3]. Therefore, accurate detection of the lymph node status is important in the staging and decision-making for the treatment.

Conventional imaging methods that include computed tomography (CT) and magnetic resonance imaging (MRI), have limited capability for LNM, with low sensitivity and accuracy, mainly because of normal-sized LNM that measure < 1 cm [4,5]. Although positron emission tomography/computed tomography (PET/CT) has higher sensitivity for detecting LNM, it has limited capability for detecting normal-sized LNM [6] and early-stage cervical cancer LNM, with a sensitivity of only 32%–58% [7]. In the literature, approximately 50–80% of LNM are normal in size [8–11]. Therefore, improving the capability for noninvasive diagnosis of normal-sized LNM will be helpful in staging and clinical decision-making.

Radiomics refers to the extraction and analysis of large amounts of advanced quantitative imaging features with high throughput from medical images [12,13]. Previous studies have demonstrated that the radiomics method might aid in diagnosing diseases and predicting treatment response and prognosis [14–17]. Recent research also demonstrated that radiomic features based on MRI, CT, and ultrasonography images can be used for predicting LNM in cervical cancer patients [18–23]. However, none of these studies focused on normal-sized LNM. In addition, although previous studies had demonstrated that the radiomic models at the patient level could improve the ability of prediction of LNM [18–23], all those studies could not localize the metastatic LNs, which meant that the previous radiomic models could just predict the LNM indirectly. Accurate prediction of the involvement in specific lymph nodes may contribute to precise resection or radiotherapy. Therefore, the purpose of this study was to develop a CT-based radiomic model and validate its usefulness for the direct prediction of normal-sized LNM in cervical cancer.

Methods

Patients

This retrospective study was approved by the institutional review board and was conducted according to the tenets of the Declaration of Helsinki and its later amendments. The requirement for informed consent was waived owing to the retrospective nature of the study. The study was conducted on 1543 patients in 10 centers from June 2008 to December 2019. The patients' inclusion criteria were as follows: (1) histologically confirmed cervical cancer; (2) history of radical hysterectomy + systematic pelvic lymph node dissection ± para-aortic lymph node dissection; (3) contrast-enhanced pelvic ± abdominal CT scans less than 2 weeks before surgery; and (4) pathologically confirmed LN status with anatomic labeling into the obturator, common iliac, internal iliac, external iliac, deep inguinal, parametrial, presacral, and para-aortic groups. The exclusion criteria were as follows: (1) combined malignancies and (2) missing necessary CT sequences on either arterial or venous phase CT images.

To ensure that the lymph node cases included in the study correspond to the pathological results in the imaging images, we have set strict inclusion criteria. All positive LNs that met the following criteria were included: (1) pathologically confirmed positive LNs in the specific anatomic regions mentioned above; (2) the number of LNs of the metastatic nodal anatomic region in the CT image is less than or equal to the number of positive LNs confirmed by pathology; and (3) the maximal short-axis diameter of the positive LNs is ≤ 1 cm in cross-sectional CT images. All negative LNs that met the following criteria were included: (1) pathologically confirmed negative LNs and (2) the maximal short-axis diameter of the negative LNs is ≤ 1 cm in cross-sectional CT images. We selected pathologically confirmed normal-sized LNs. Thus, some of the included patients may have multiple LNs.

In total, 273 LNs of 219 patients from 10 centers were included in the final study. We selected 2 centers (Nanfang Hospital, Southern Medical University; Affiliated Hospital of Qingdao University) with the largest number of LNs and randomly divided them into the training and internal validation cohorts in a 2:1 ratio. The LNs in the remaining 8 centers were classified into the external validation cohort. It was worth noting that the training cohort was used for training the predicting model and the internal validation cohort was performed to adjust the parameters. Moreover, we used the external validation cohort to evaluate the performance and generalization ability of the model. The details are listed in Supplementary Table S1.

Image acquisition, segmentation, and radiomic feature extraction

We retrieved CT images from the picture archiving and communication system. All images were derived in the Digital Imaging and Communications in Medicine format. Manual segmentation of the arterial and venous phase CT images was performed on ITK-SNAP software (version 3.6.8; www.itksnap.org) and included LNs were defined as regions of interest (ROIs). The target images were delineated by one gynecologist with 5 years of experience (reader1) in pelvic CT diagnosis. Each slice of the CT image was normalized by using the z-score to obtain a standard normal distribution of image intensities [24,25]. Features, including first-order (intensity) features, texture features, and shape features, were extracted from ROIs of the arterial and venous phase CT images using a Pyradiomic package in Python 3.6 software (http://www.python.org/) [26]. Then, the radiomic features in the three cohorts were standardized.

To evaluate the intra- and inter-observer agreement, thirty LNs from arterial and venous phase CT images were randomly selected from the dataset. We invited reader1 and another experienced gynecologist (reader2) to independently segment the ROIs again. The intraclass correlation coefficient (ICC) was calculated. The radiomic features with ICCs>0.75 were considered to be robust and consistent.

Model building

All the analyses were based on the training cohort and optimized to the best performance in the internal validation cohort and tested in the external validation cohort. In the univariate analysis, we saved the radiomic features separately which were significantly related to the LNM in each phase as input for further analysis [27].

Fig 1 is the workflow of the model construction. Feature selection and classifiers were common and effective methods for establishing diagnostic models [21,24–26,31]. Unlike those methods, single-phase models were developed by the artificial neural network (ANN) with 5 fully connected layers by using the features of corresponding single-phases. Then, a radiomic model was generated by the linear combination of the arterial and venous single-phase models. Moreover, as exhibited in Supplementary A1, we also used four different state-of-the-art

Table 1
The characteristics in the three cohorts.

Index	Training cohort		Internal validation cohort		External validation cohort	
	Positive	Negative	Positive	Negative	Positive	Negative
OLN	20	60	14	33	0	30
IILN	5	6	1	4	0	3
PLN	5	0	2	0	1	0
CILN	5	8	3	1	2	1
EILN	12	22	1	9	2	9
DILN	1	4	2	4	0	3
Total	48	100	23	51	5	46

OLN, obturator LN; IILN, internal iliac LN; EILN, external iliac LN; CILN, common iliac LN; DILN, deep inguinal LN; PLN, parametrial LN.

methods to build and compare single-phase models and combined models.

Statistical analysis

The performance of the models we built was validated according to the area under the receiver operating characteristic (ROC) curves (AUC). The specificity, sensitivity, and accuracy were also calculated. Additionally, a decision curve analysis was performed for the model with the best performance. The best performing model was also subjected to a stratified analysis to evaluate its predictive capability under different anatomic regions of LNs.

In a univariate analysis, the Mann-Whitney U test was adopted for testing the potential correlation of the radiomic features and LNM in the training cohort. Two-sided *P* values of < 0.05 were considered statistically significant. All statistical analyses were performed by using *R* software (version 3.5.3). The ANN models were constructed through Python (version 3.6.5, https://www.python.org/) using the Pytorch package (https://www.pytorch.org/).

Results

Patient characteristics

Supplementary Fig 1 illustrates the procedure of data selection. There were 76 positive LNs and 197 negative LNs (Table 1). In the training cohort, 32.4% (48/148) of the LNs were positive and 67.6% (100/148) were negative. In the internal validation cohort, 31.1% (23/74) of the LNs were positive and 68.9% (51/74) were negative. In the external validation cohort, 9.8% (5/51) of the LNs were positive and 90.2% (46/51) were negative. The clinicopathologic characteristics of the patients are given in Supplementary Table S2.

Model construction

A total of 1409 features were extracted from each phase of the CT image.

Those features demonstrated good consistency. The ICCs of 1339 features (95.03%) from arterial images and 1330 features (94.39%) from venous images were greater than 0.75, and therefore, those robust features were applied for further analysis. There were 190 and 374 radiomic features from the arterial phase and venous phase, respectively, which were significantly correlated with LNM in univariate analysis (*P* < 0.05).

As demonstrated in Supplementary Fig 2 and Table S4–6, we found that the models we built had good performance for predicting LNs in cervical cancer. Moreover, the combined models integrating two-phase images surpassed the single-*p*hase models and the venous phase models were better than arterial models. The models built by ANN were higher than those models developed by other methods. Detailed information

about those four methods is given in Supplementary A2. Table 2 illustrates the performance of the three models generated by ANN.

The radiomic model exhibited the optimal distinguishing capability with the AUCs of 0.912 (95% CI: 0.862–0.963) and 0.859 (95% CI: 0.776–0.941) in the training and internal validation cohorts (Fig 2). The decision curve analyses of the radiomic model are illustrated in Fig 3a. There was a significant difference in the distribution of predicted values of the radiomic model between positive and negative LNs (Figs 3b and 4).

Clinical analysis

In our study, the LNs we included could be further subdivided into the obturator LN (OLN), internal iliac LN (IILN), external iliac LN (EILN), common iliac LN (CILN), deep inguinal LN (DILN), and parametrial LN (PLN). Thus, we stratified the LNs into two groups: group 1 including OLN, IILN, and PLN; and group 2 including CILN, EILN, and DILN. The predictive capability of the radiomic model under the different anatomic regions of LNs is illustrated in Fig 3c. We found no significant difference in the discrimination performance of the radiomic model between group 1 and group 2 (*P* = 0.011).

Discussion

Using a multicenter data set, we successfully developed and validated a radiomic model based on CT imaging features in the arterial and venous phases to discriminate between positive and negative LNs of normal size in cervical cancer patients.

LNM is a negative prognostic factor for patients with cervical cancer. Noninvasive prediction of the LN status in patients with cervical cancer is important to develop a personalized treatment strategy. The conventional methods for evaluating the LN status include CT and MRI, which determined the LN status mostly depending on the morphologic appearance of the LN [28]. Primarily, LNM is diagnosed when the short-axis diameter of the LN is > 1 cm [29]. However, Benedetti et al. reported that among cervical cancer patients with positive LNs, the diameter of metastatic nodes was < 1 cm in 86.5% (333/385) [8]. Another study depicted that in patients with gynecologic tumors, 54.5% of positive LNs were less than 1 cm in diameter [9]. Normal-sized LNM is common, but there are few noninvasive methods to identify them. An accurate diagnosis of normal-sized LNM might be helpful for preoperative staging. Furthermore, it might help with precision resection of the metastatic nodes or implement individualized radiotherapy in patients with positive LNs. Therefore, it is important to improve the performance of noninvasive methods for detecting normal-sized LNM.

Radiomics has rapidly evolved in recent years, and it may provide quantitative and objective data that can be helpful for decision-making about cancer detection and treatment [30,31]. Several studies have reported that the radiomic signature from CT, MRI, or ultrasound images has favorable capability in predicting LNM in cervical cancer [18–23]. Radiomic models based on MR images have reported AUCs ranging from
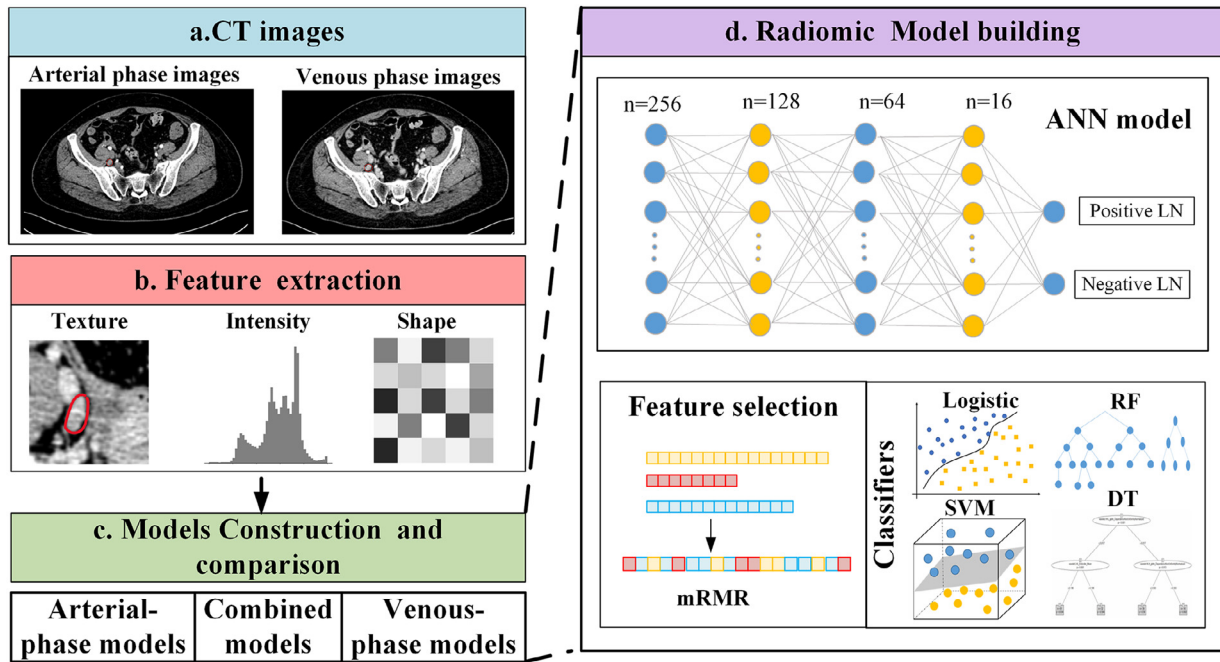
Fig 1. Workflow of the model construction. (a) CT images from arterial and venous phases. (b) Features including shape, intensity, and texture, extracted from the two phases. (c) Arterial and venous phase models and combined models were built. (d) We constructed the radiomic model by ANN with 5 fully connected layers. The feature selection method and different classifiers were used for modeling and comparison. mRMR, minimum redundancy maximum relevance; SVM, support vector machine; DT, decision tree; RF, random forest; ANN, artificial neural network.

Table 2

Performance of the radiomic model.

Index	Specificity	Sensitivity	Accuracy	AUC (95% CI)	TN	TP	FN	FP
Venous phase model								
Training	0.900	0.812	0.872	0.894 (0.832-0.956)	90	39	9	10
Internal validation	0.784	0.739	0.770	0.853 (0.768-0.939)	40	17	6	11
External validation	0.652	1.000	0.686	0.835 (0.675-0.995)	30	5	0	16
Arterial phase model								
Training	0.830	0.729	0.797	0.781 (0.692-0.870)	83	35	13	17
Internal validation	0.784	0.696	0.757	0.734 (0.598-0.870)	40	16	7	11
External validation	0.891	0.400	0.843	0.678 (0.466-0.934)	41	2	3	5
Radiomic model								
Training	0.890	0.854	0.878	0.912 (0.862-0.963)	89	41	7	11
Internal validation	0.765	0.870	0.797	0.859 (0.776-0.941)	39	20	3	12
External validation	0.739	0.8	0.745	0.800 (0.667-0.933)	34	4	1	12

TN, true negative; TP, true positive; FN, false negative; FP, false positive.

Fig 2. AUCs of all the models we constructed in the internal validation cohort.
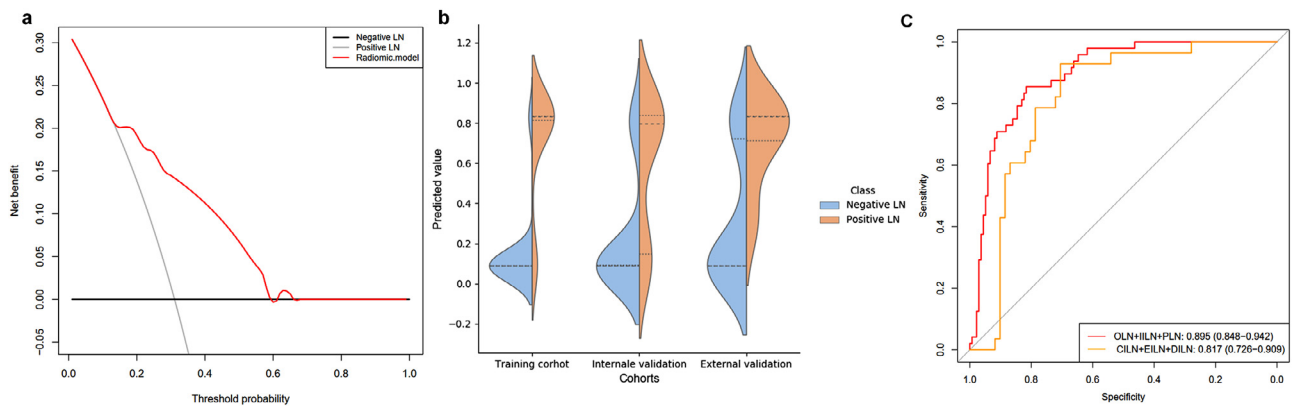
Fig 3. (a) Decision curve of the radiomic model. (b) The distribution of the predicted values of the radiomic model in three cohorts. (c) ROC curves of different anatomic regions of LNs in the radiomic model.
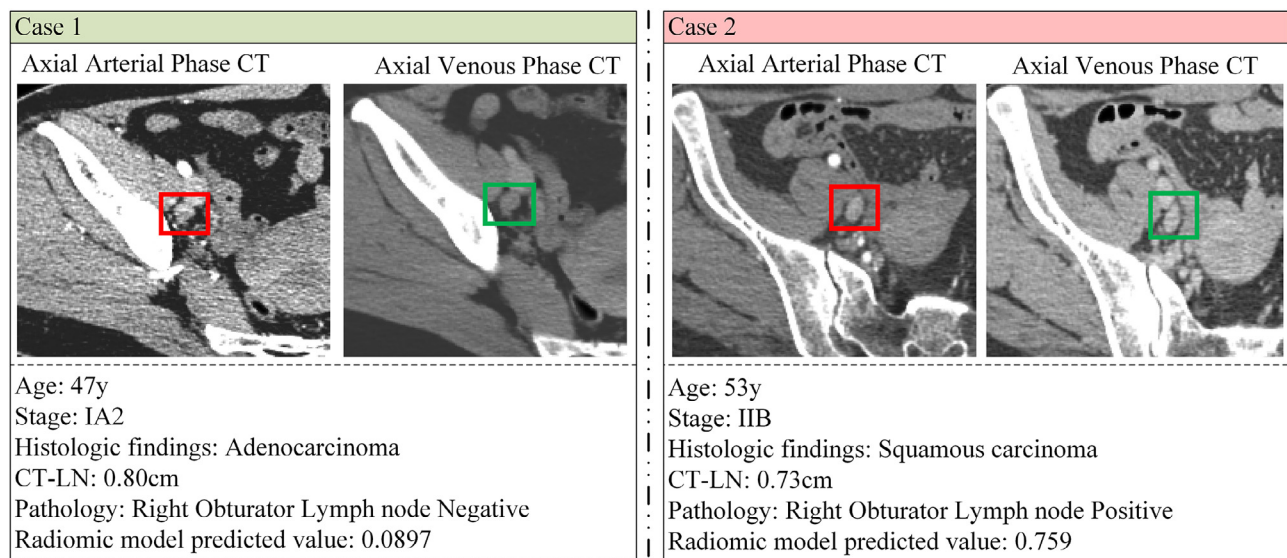
Fig 4. Two examples of the combined model for predicting lymph node metastasis.

0.754 to 0.922 [18–20,23]. Chen et al. also reported a CT-based radiomic model with acceptable predictive values for LNM in cervical cancer patients, with the AUC of 0.80 in the training cohort and 0.75 in the validation cohort [21]. In addition, Jin et al. reported the feasibility of the use of radiomic features from ultrasound images [22]. Although these studies demonstrated that the radiomic features might help to discriminate patients with positive LNs from those with negative LNs, none of these focused on normal-sized metastatic LNs. Moreover, the prediction models mentioned above could only indirectly define the presence of LNM in patients, but could not pinpoint the specific positive LNs, which was insufficient in the precision resection or radiation of the metastatic nodes. Sha et al. demonstrated that radiomic features of mediastinal LNs on CT images exhibited acceptable ability in predicting the involvement of LNs in non-small-cell lung cancer patients [32]. Their study indicated that radiomic features might be different between positive and negative LNs, and these distinguishing features might be useful for directly predicting the involvement in specific LNs.

In this study, a radiomic model for diagnosing a normal-sized LNM in cervical cancer was built by comparison. The models based on venous phase CT images demonstrated better performance than those models based on arterial phase images. This could be because the arterial phase mainly reflects blood perfusion of tumor tissues, whereas the venous phase reflects blood clearance, which is an important imaging feature of tumor metastasis [33]. Perfusion CT imaging can provide an oppor-

tunity to quantify tumor heterogeneity (e.g. blood flow, blood volume, permeability, and mean transit time) [34]. Our results indicated a more significant heterogeneity between positive and negative LN in the venous phase. In addition, the models combining the features of the two phases demonstrated better discrimination capability than the single-phase models regardless of the method of model construction. This result indicated that arterial and venous phase radiomic features play a synergistic role in predicting normal-sized LNM. The models constructed by using ANN outperformed those carried out by the other four methods, demonstrating that the ANN model could make full use of all the extracted features and discovered the potential relationship between them.

The radiomic model in our study achieved the highest AUCs of 0.912 and 0.859 in the training and internal validation cohorts, respectively, and these were higher than or equal to those in previous studies [18,21,22]. Another advantage of our study was that we only included normal-sized LNs, so that our model can focus on each LN, particularly the suspicious LNs, and realize an accurate diagnosis. In addition, the radiomic model had better sensitivity (0.854 and 0.870 in the training and internal cohort, respectively) than that of models in previous studies [18,21,22]. The high sensitivity, which was equal to a low false-negative rate, might be beneficial for staging and clinical decision-making in patients with normal-sized LNM. In the external validation cohort, the radiomic model remained to exhibit good performance, with an AUC of 0.800. This indicated that the model had acceptable generalization ca-

pability. In addition, we applied the decision curve analysis to assess whether the radiomic model-assisted decisions would improve patient outcomes. Our results demonstrated that the radiomic model was more beneficial than either the treat-all or the treat-none strategy indicating good clinical usefulness.

The morphologies of pelvic lymph nodes were different from region to region. To test the feasibility of the radiomic model under different anatomical regions, we divided the LNs into 2 groups in accordance with the anatomical region for the stratified analysis. The AUC value of the radiomic model was 0.90 in group 1 and 0.82 in group 2, suggesting that the prediction model was applicable for evaluating LNs in all anatomical regions.

This study also had some limitations. First, the clinical data was insufficient. The discrimination capacity of the combined clinical information and imaging features could not be evaluated. Previous studies have demonstrated that combined models which included clinical information and radiomic features outperformed the radiomic models [23]. Hence, more effective clinical characteristics will be enrolled in future studies at the patient level. Second, plain-phase CT images were not enrolled in our study. Thus, we need to collect more plain-phase CT images and evaluate the feasibility of the plain CT radiomic model for predicting normal-sized LNM in cervical cancer in the future. Third, this study used images from different CT scanners, and the impact of the types of CT scanner and CT scanning parameters should be further studied. Finally, although this was a multicenter data analysis, the number of samples was relatively small. Future studies should include a higher number of cases and a balance between the number of negative and positive cases to further validate the reliability of our model for clinical application.

Conclusion

In conclusion, we developed and validated a radiomic model incorporating the arterial and venous phase CT features for a noninvasive, directly diagnosed, normal-sized LNM in cervical cancer patients. The radiomic model achieved an excellent validation result in this study, and to some extent, it could assist clinicians in clinical staging and decision-making.

Declaration of Competing Interest

The authors declare no conflicts of interest.

CRediT authorship contribution statement

Yujia Liu: Conceptualization, Formal analysis, Investigation, Methodology, Software, Writing - original draft, Writing - review & editing. **Huijian Fan:** Conceptualization, Data curtion, Formal analysis, Investigation, Methodology, Writing - original draft, Writing - review & editing. **Di Dong:** Conceptualization, Formal analysis, Investigation, Methodology, Writing - review & editing, Funding acquisition. **Ping Liu:** Data curtion, Investigation, Writing - review & editing. **Bingxi He:** Formal analysis, Methodology, Software, Validation, Visualization. **Lingwei Meng:** Formal analysis, Methodology, Software, Validation, Visualization. **Jiaming Chen:** Data curtion, Investigation, Writing - original draft. **Chunlin Chen:** Data curtion, Funding acquisition, Writing - review & editing. **Jinghe Lang:** Data curtion, Investigation, Resources, Supervision. **Jie Tian:** Funding acquisition, Methodology, Resources, Supervision.

Acknowledgments

Supplementary materials

Supplementary material associated with this article can be found, in the online version, at doi:10.1016/j.tranon.2021.101113.

References

[1] M. Arbyn, E. Weiderpass, L. Bruni, et al., Estimates of incidence and mortality of cervical cancer in 2018: a worldwide analysis, Lancet Glob. Health 8 (2) (2020) e191–e203.

[2] L.T. Gien, A. Covens, Lymph node assessment in cervical cancer: prognostic and therapeutic implications, J. Surg. Oncol. 99 (4) (2009) 242–247.

[3] N. Bhatla, J.S. Berek, M.C. Fredes, et al., Revised FIGO staging for carcinoma of the cervix uteri, Int. J. Gynecol. Obstetr. 145 (1) (2019) 129–135.

[4] J. Scheidler, H. Hricak, K.K. Yu, L. Subak, MR. Segal, Radiological evaluation of lymph node metastases in patients with cervical cancer. a meta-analysis, Jama 278 (13) (1997) 1096–1101.

[5] H.J. Choi, W. Ju, S.K. Myung, Y. Kim, Diagnostic performance of computer tomography, magnetic resonance imaging, and positron emission tomography or positron emission tomography/computer tomography for detection of metastatic lymph nodes in patients with cervical cancer: meta-analysis, Cancer Sci. 101 (6) (2010) 1471–1479.

[6] J.Y. Park, J.J. Lee, H.J. Choi, et al., The value of preoperative positron emission tomography/computed tomography in node-negative endometrial cancer on magnetic resonance imaging, Annal. Surg. Oncol. 24 (8) (2017) 2303–2310.

[7] A. Torigian D, D. Sahra Emamzadehfard M, D. Koosha Paydary M, et al., Update of the role of PET/CT and PET/MRI in the management of patients with cervical cancer, Hellenic J. Nucl. Med. 19 (3) (2016) 254–268.

[8] P. Benedetti-Panici, F. Maneschi, G. Scambia, et al., Lymphatic spread of cervical cancer: an anatomical and pathological study based on 225 radical hysterectomies with systematic pelvic and aortic lymphadenectomy, Gynecol. Oncol. 62 (1) (1996) 19–24.

[9] A.D. Williams, C. Cousins, W.P. Soutter, et al., Detection of pelvic lymph node metastases in gynecologic malignancy: a comparison of CT, MR imaging, and positron emission tomography, Am. J. Roentgenol. 177 (2) (2001) 343–348.

[10] S. Tangjitgamol, S. Manusirivithaya, C. Sheanakul, et al., Can we rely on the size of the lymph node in determining nodal metastasis in ovarian carcinoma? Int. J. Gynecol. Cancer 13 (3) (2003).

[11] S. Tangjitgamol, S. Manusirivithaya, S. Jesadapatarakul, et al., Lymph node size in uterine cancer: a revisit, Int. J. Gynecol. Cancer 16 (5) (2006) 1880–1884.

[12] P. Lambin, E. Rios-Velazquez, R. Leijenaar, et al., Radiomics: extracting more information from medical images using advanced feature analysis, Eur. J. Cancer 48 (4) (2012) 441–446.

[13] V. Kumar, Y. Gu, S. Basu, et al., Radiomics: the process and the challenges, Magn. Reson. Imaging 30 (9) (2012) 1234–1248.

[14] HJ. Aerts, The potential of radiomic-based phenotyping in precision medicine: a review, JAMA Oncol. 2 (12) (2016) 1636–1642.

[15] R.J. Gillies, P.E. Kinahan, H. Hricak, Radiomics: images are more than pictures, they are data, Radiology 278 (2) (2016) 563–577.

[16] Z. Liu, S. Wang, J.W. Di Dong, et al., The applications of radiomics in precision diagnosis and treatment of oncology: opportunities and challenges, Theranostics 9 (5) (2019) 1303.

[17] D. Dong, L. Tang, Z.Y. Li, et al., Development and validation of an individualized nomogram to identify occult peritoneal metastasis in patients with advanced gastric cancer, Ann. Oncol. 30 (3) (2019) 431–438.

[18] Y. Kan, D. Dong, Y. Zhang, et al., Radiomic signature as a predictive factor for lymph node metastasis in early-stage cervical cancer, J. Magn. Reson. Imaging 49 (1) (2019) 304–310.

[19] T. Wang, T. Gao, J. Yang, et al., Preoperative prediction of pelvic lymph nodes metastasis in early-stage cervical cancer using radiomics nomogram developed based on T2-weighted MRI and diffusion-weighted imaging, Eur. J. Radiol. 114 (2019) 128–135.

[20] Q. Wu, S. Wang, X. Chen, et al., Radiomics analysis of magnetic resonance imaging improves diagnostic performance of lymph node metastasis in patients with cervical cancer, Radiother. Oncol. 138 (2019) 141–148.

[21] J. Chen, B. He, D. Dong, et al., Noninvasive CT radiomic model for preoperative prediction of lymph node metastasis in early cervical carcinoma, Br. J. Radiol. 93 (1108) (2020) 20190558.

[22] X. Jin, Y. Ai, J. Zhang, et al., Noninvasive prediction of lymph node status for patients with early-stage cervical cancer based on radiomics features from ultrasound images, Eur. Radiol. 30 (7) (2020) 4117–4124.

[23] M. Xiao, F. Ma, Y. Li, et al., Multiparametric MRI-based radiomics nomogram for predicting lymph node metastasis in early-stage cervical cancer, J. Magn. Reson. Imaging 52 (3) (2020) 885–896.

[24] D. Dong, F. Zhang, L.Z. Zhong, et al., Development and validation of a novel MR imaging predictor of response to induction chemotherapy in locoregionally advanced nasopharyngeal cancer: a randomized controlled trial substudy (NCT01245959), BMC Med. 17 (1) (2019) 190.

[25] L. Meng, D. Dong, X. Chen, et al., 2D and 3D CT radiomic features performance comparison in characterization of gastric cancer: a multi-center study, IEEE J. Biomed. Health Inform. 25 (3) (2021) 755–763.

[26] Q. Li, Y. Liu, D. Dong, et al., Multiparametric MRI radiomic model for preoperative predicting WHO/ISUP nuclear grade of clear cell renal cell carcinoma, J. Magn. Reson. Imaging 52 (5) (2020) 1557–1566.

[27] H. Peng, D. Dong, M.J. Fang, et al., Prognostic value of deep learning PET/CT-based radiomics: potential role for future individual induction chemotherapy in advanced nasopharyngeal carcinoma, Clin. Cancer Res. 25 (14) (2019) 4271–4279.

[28] S. Ganeshalingam, D-M. Koh, Nodal staging, Cancer Imaging 9 (1) (2009) 104–111.

[29] M. Follen, C.F. Levenback, R.B. Iyer, P.W. Grigsby, E.A. Boss, E.S. Delpassand, B.D. Fornage, EK. Fishman, Imaging in cervical cancer, Cancer 98 (9 Suppl) (2003) 2028–2038.

[30] P. Lambin, R.T.H. Leijenaar, T.M. Deist, et al., Radiomics: the bridge between medical imaging and personalized medicine, Nat. Rev. Clin. Oncol. 14 (12) (2017) 749–762.

[31] D. Dong, M.J. Fang, L. Tang, et al., Deep learning radiomic nomogram can predict the number of lymph node metastasis in locally advanced gastric cancer: an international multi-center study, Ann. Oncol. 31 (7) (2020) 912–920.

[32] X. Sha, G. Gong, Q. Qiu, J. Duan, D. Li, Y. Yin, Discrimination of mediastinal metastatic lymph nodes in NSCLC based on radiomic features in different phases of CT imaging, BMC Med. Imaging 20 (1) (2020) 12.

[33] T. Perrin, A. Midya, R. Yamashita, et al., Short-term reproducibility of radiomic features in liver parenchyma and liver malignancies on contrast-enhanced CT imaging, Abdom. Radiol. 43 (12) (2018) 3271–3278.

[34] B. Ganeshan, KA. Miles, Quantifying tumour heterogeneity with CT, Cancer Imaging 13 (2013) 140–149.